Engineered bacterial M1GS ribozyme efficiently cleaves the most abundant ribosomal RNA in a human cancer cell line

Neha Priyadarshini[1†], Navinchandra Venkatarama Puppala[2†], Harikrishnan Poiyamozhi[1], Swati Biswas[3], and Gireesha Mohannath[1*]

[1]Department of Biological Sciences, Birla Institute of Technology & Science-Pilani, Hyderabad Campus, Hyderabad, Telangana, India.

[2]Institute for Developmental Biology and Neurobiology, Johannes Gutenberg University Mainz, Biozentrum I, Mainz, Germany

[3]Department of Pharmacy, Birla Institute of Technology & Science-Pilani, Hyderabad Campus, Hyderabad, Telangana, India.

† These authors contributed equally to this work

*Correspondence:

Email: gireesha@hyderabad.bits-pilani.ac.in

Abstract

M1GS, an engineered Ribonuclease P (RNase P), can be customized to specifically target and cleave any RNA. It involves tethering an *Escherichia coli* M1 RNA to a short guide sequence (GS) complementary to the RNA targeted for cleavage. We have developed a Python script-based bioinformatic tool built based on the requirements of M1GS, coupled to secondary structure predictions, to identify M1GS target sites for any given RNA. Primarily, we demonstrate the utility of the tool for predicting M1GS target sites across multiple RNAs, including human 28S ribosomal RNA (rRNA), and then we demonstrate efficient M1GS-mediated downregulation of 28S rRNA in a human cancer cell line. Efficient cleavage of rRNA, the most abundant RNA molecule, suggests a high turnover number for the M1GS ribozyme. Lastly, we discuss the utility of M1GS ribozyme-mediated rRNA downregulation as a potential anticancer modality in cancers where rRNAs are upregulated.

Keywords

RNase P ribozyme, M1GS ribozyme, M1GS target site finder, RNA cleavage, human 28S rRNA, gene knockdown

72 **Introduction**

73 Targeted RNA cleavage has commonly been employed as a reverse-genetic tool to
74 understand genes' functions and as a defense modality against pathogens, including viruses.
75 Commonly used tools include RNA interference (RNAi)/antisense RNA [1-4], engineered
76 ribozymes [5], and recently developed CRISPR-Cas-based genome editing tools [6, 7].

77 Ribonuclease P (RNase P) RNA is among the earliest discovered ribozymes and is a
78 ribonucleoprotein (RNP) complex found in all three domains of life [8, 9]. Although RNase P
79 has a shared function in the 5' tRNA maturation, the composition of the RNase P RNP complex
80 is evolutionarily divergent [10-15]. In *Escherichia coli*, RNase P is made up of a catalytic RNA
81 component called M1 RNA and a protein cofactor called C5 [16-18]. M1 RNA possesses
82 catalytic activity *in vitro* in the absence of a protein cofactor [19]. RNase P recognizes
83 precursor tRNA based on its structure, not the tRNA sequence. This feature was explored to
84 engineer RNase P to selectively target and cleave any RNA molecule as a gene knockdown
85 strategy [9, 20-22].

86 M1GS is an RNase P-based gene knockdown strategy, wherein *E. coli* M1 RNA is
87 fused through its 3' end to a guide sequence (GS), which is complementary to the target RNA.
88 When the customized M1GS is expressed in the transfected cells, the GS hybridizes to the
89 complementary sequence in the target RNA which is then cleaved by the tethered M1 RNA
90 immediately upstream of the binding site (Figure 1) [15, 23, 24]. The M1GS strategy has been
91 used to downregulate genes in both prokaryotes and eukaryotes, demonstrating its utility as
92 an effective tool for disrupting genes' functions [25-27]. Moreover, the M1GS strategy is
93 simple, consisting of the expression of a single exogenous M1 RNA fused to a few short
94 sequences. Its total length, including all the sequences expressed, is ~590 nt. Further, it can
95 be expressed using various types of inducible and constitutive promoters [28, 29]. An inactive
96 M1GS carrying an enzymatically deficient mutant version of the M1 RNA has been included
97 in multiple studies as a control to demonstrate that the mutant phenotype observed in their
98 studies is due to the enzymatically active M1GS-mediated cleavage, not due to the GS-target
99 RNA base-pairing or any other random effects of the M1GS expression [23, 26, 27, 30].
100 However, despite its simplicity, specificity, and effectiveness in cleaving targeted RNA, the
101 M1GS strategy appears to be underutilized. Perhaps one reason is that prior knowledge of
102 the M1GS target site requirements is necessary for its use, discouraging its frequent use.

103 Although M1GS has been employed to cleave multiple RNAs in human cells, it has not
104 been tested to cleave ribosomal RNA (rRNA), the most abundant RNA species (up to 80% of
105 total RNA). In the nucleolus, RNA polymerase I (RNA Pol I) transcribes 45S rRNA genes to
106 produce pre-45S rRNA, which is then processed to 18S, 5.8S, and 28S rRNAs, which form
107 the catalytic core of ribosomes, the protein-synthesising cell organelles (Figure S1). 45S

108 ribosomal RNA genes are upregulated in several cancers [31-33], and therefore, RNA Pol I
109 transcription has been therapeutically targeted in these cancers [34-40].
110 In this study, we describe *M1GS Target Site Finder*, a Python script-based user-
111 friendly bioinformatic tool we developed to identify M1GS target sites for any given RNA using
112 either DNA or RNA sequence as input. We demonstrate the utility of this bioinformatic tool in
113 predicting M1GS target sites for multiple RNAs, including human 28S rRNA. Then, we
114 demonstrate its downregulation via targeted cleavage by a customized M1GS ribozyme in a
115 lung cancer cell line, using one of the GSs identified by the tool. Lastly, we discuss the potential
116 advantages of M1GS ribozyme and M1GS ribozyme-mediated rRNA downregulation as a
117 potential anticancer modality in cancers where rRNAs are upregulated.
118
119 **Results**
120 We developed a Python script-based bioinformatic tool with a user-friendly web interface for
121 automated identification of all possible M1GS cleavage sites for any target RNA. It provides
122 the flexibility to customize the need-based predictions with various input options. A flowchart
123 depicting the workflow of the *M1GS target finder* tool is shown in Figure 2. The tool can be
124 accessed using the link (http://m1gstargetfinder.bits-hyderabad.ac.in:8000/m1gs/). Several
125 input options that an end user can provide are described below. All the recommended input
126 options are for M1GS involving *E. coli* M1 RNA only. Users have to determine if these options
127 work equally well for other RNase P RNA.
128
129 **Inputs for *M1GS target site finder* tool**
130 **Sequence of the target RNA**
131 To identify all M1GS sites in a target RNA, as the first step, the sequence of the target RNA
132 or DNA should be entered in the given space in the tool where it asks for 'Sequences of target
133 RNA/DNA'. If users provide a DNA sequence as input, the tool will automatically convert it to
134 the corresponding RNA sequence and then use it to identify M1GS target sites.
135
136 **The nucleotide at the -1 position**
137 The 5' nucleotide with respect to the M1GS cleavage site (-1 position) is a pyrimidine [15, 24].
138 Uracil is a conserved preference at the -1 position of the pre-tRNA in bacteria and archaea
139 [41]. Consistent with this conservation, U at the -1 position was found to be critical for cleavage
140 site selection and cleavage efficiency of tRNA substrates [42]. However, some bacterial
141 species also have adenine, cytosine, or guanine at the -1 position, demonstrating that
142 cleavage is also possible with nucleotides other than uracil at -1. Several studies have
143 demonstrated customized M1GS-mediated cleavage of the target mRNA with varying
144 nucleotides at the -1 position [43-45]. Therefore, we designed our tool to provide a choice of

all four nucleotides at the -1 position. End users are recommended to prefer uracil at the -1 position, but if it is unavailable, they may choose cytosine (the other pyrimidine) or any other nucleotides of their choice.

The nucleotide at the +1 position

The identity of the base at the +1 position is a salient determinant for the M1GS cleavage site selection. A purine at the +1 position is important for both cleavage efficiency and cleavage site selection (between the -1 and +1 sites), regardless of whether the +1 nucleotide is base-paired or not [24]. When a purine at the +1 position is base-paired, it results in optimal cleavage of the target RNA [24]. In contrast, when a pyrimidine is at the +1 position and is not base-paired, it results in an aberrant cleavage [24]. Moreover, cleavage of a substrate with a purine at the +1 position is more efficient than with a pyrimidine at the +1 position. Therefore, a purine nucleotide at the +1 position is a dominant determinant for M1GS cleavage site selection and cleavage efficiency. This observation is consistent with the notion that a guanine at the +1 position, which has been found in most bacterial pre-tRNAs, serves as the guide nucleotide for M1 RNA and RNase P cleavage in *E. coli* [24]. To meet this requirement, we have provided an option in the tool to choose either purine (A or G) at the +1 position.

Length of the desired GS

The optimal length of the GS can vary from 12-19 nt [23], although M1GS can cleave shorter RNA substrates [24]. The longer the length of a GS, the higher the specificity of the M1GS targeting but as the GS length increases, the turnover number of the M1GS ribozyme may be negatively impacted due to tighter M1GS binding to the target RNA. By contrast, shorter GSs may lead to an enhanced M1GS turnover number but could result in more off-target cleavages. In addition to the length of GS, the GC% of GS also contributes to the M1GS ribozyme cleavage efficiency because GC% determines the strength of base-pairing. For these reasons, the users may try GSs of different lengths if they deem necessary. Based on the length of the guide sequence chosen (excluding 3' NCCA), target sites of an equal length in the target RNA will be predicted. Note that the length of GS does not change the positions or number of the M1GS target sites in the target RNA.

The desirable length of the GS-binding target RNA from the -1 position to be in a single-stranded configuration

For M1GS to efficiently bind and cleave the target RNA, it is preferable to choose a region of the target RNA that is likely to exist in a single-stranded form. To identify such regions in the target RNA, past studies have used chemical methods [23, 30] and prediction software [25, 27]. The *M1GS target site finder* tool is linked to the publicly available RNAfold software tool

182 (http://rna.tbi.univie.ac.at/cgi-bin/RNAWebSuite/RNAfold.cgi). The tool, by default, uses the
183 RNAfold-predicted secondary structure of the target RNA, which is then used to identify
184 regions in the target RNA that are predicted to exist in accessible conformation. The default
185 settings of the RNAfold tool used for secondary structure prediction are shown in Figure S2.
186 Alternatively, the users can provide RNA secondary structure input in Vienna format obtained
187 from any other RNA secondary structure prediction tool of their choice.
188 To find such desirable target RNA sites, users should provide a desirable length of the
189 GS-binding target RNA from the -1 position to be in a single-stranded configuration as an
190 input. For example, if the length of the GS is 14 nt, one can start by providing the input
191 specifying the desirable length of the target RNA in a single-stranded form as 14 nt. Although
192 it is desirable to use target RNA sites that would likely exist in a single-stranded form *in vivo*,
193 it is often not possible to find such ideal sites in target RNAs based on the *in silico* secondary
194 structure prediction. M1GS could still bind and cleave such RNAs [23, 25]. Therefore, if no
195 target sites are found with the desired target RNA length in a single-stranded form, the end
196 user is recommended to keep reducing the required length until a minimum number of desired
197 target sites is found. In cases where the software predicts that no region of the input RNA
198 sequence that matches M1GS requirements exists in a single-stranded configuration, the
199 input for the desirable length of a single-stranded target RNA can be put at '0'. The M1GS
200 could still cleave such targets, although it might affect cleavage efficiency. The reasoning is
201 that the secondary structures predicted by software may not reflect the exact *in vivo* scenarios.
202 Therefore, GSs may still bind and cleave such target sites [23, 25]. Alternatively, the predicted
203 RNA secondary structures may be weak and thus could be disrupted in the presence of the
204 customized M1GS RNA, favoring the base-pairing between the target RNA and the M1GS.
205 The overall approach to choosing this or the other features could be to start with the ideal
206 combination of features and start relaxing the non-essential features as needed, depending
207 upon the output. Alternatively, the users could also start with relaxed features first and then
208 keep increasing the stringency until the desired M1GS target sites are found.
209
210 **Secondary structure of the target RNA**
211 Providing the secondary structure of the target RNA is an optional field in the tool. If this field
212 is left empty, the tool uses the RNAFold web server by default to predict the secondary
213 structure of the target RNA from the given input sequence (DNA or RNA). If secondary
214 structure predictions from other software are used, they should be entered in the Vienna
215 format in the specified input space in the tool. For example, another RNA folding prediction
216 software, Mfold, provides the secondary structure output in multiple formats, including the
217 Vienna format, which is suitable for this tool. Often, different prediction software give different

218 predicted secondary structures for the same RNA sequence, as demonstrated below in the
219 Results and Discussion sections.
220
221 **Unpaired nucleotide at the -1 position**
222 In consistent with the recommended unpaired RCCA or NCCA at the 3' end of GS [15, 46-48],
223 we have an additional feature to choose if the nucleotide at the -1 position, as per the predicted
224 secondary structure, is base-paired or free. The purpose is to keep the cleavage site on the
225 target RNA in a single-stranded form, as base-pairing of the nucleotide at the -1 position may
226 act as a structural anti-determinant affecting cleavage rate and specificity [49]. However,
227 cleavage can occur even when the nucleotide at the -1 position is paired [25], but cleavage
228 efficiency may be low in such cases.
229
230 **Unpaired CCA-3'**
231 To mimic *E. coli* pre-tRNA substrates, an unpaired RCCA or NCCA is added at the 3' end of
232 the M1GS RNA [15, 46-48]. Similar to the nucleotide at the -1 position, keeping CCA unpaired
233 is desirable for efficient cleavage and site selection [49]. The reason is that base-pairing of
234 this CCA with one of the M1 RNA domains is essential for catalytic activity and site selection.
235 This base-pairing would get impeded if 3' CCA base-pairs with the target RNA [49]. Therefore,
236 we recommend users to choose unpaired CCA at the 3' end, but still provide an option in our
237 tool to identify sites without unpaired 3' CCA if desired by users for some experimental
238 reasons.
239
240 **Avoiding off-target effects**
241 The M1GS target sites chosen to cleave a target RNA should ideally be unique to avoid off-
242 target effects. To avoid off-target effects, the user is recommended to verify that the chosen
243 target site(s) do not hybridize with any other RNAs in the targeted cell type, using available
244 relevant bioinformatic tools.
245
246 **Running the tool**
247 Upon entering the input RNA sequence (with or without secondary structure data) and
248 selected the desired features of the GS and the target RNA, the user can run the tool by
249 clicking 'find target sites'.
250
251 **Output**
252 The output provides a list of all possible M1GS target sites based on the provided inputs. The
253 list consists of three components: target sites with a specific nucleotide at the -1 position (e.g.,

254 U) in the target RNA, the target site sequences (from the +1), and the GC content of the target
255 sites, as described below with screenshots from the tool.
256
257 **Target site selection and designing guide sequence**
258 M1GS can be employed to cleave both coding and non-coding RNA. If the mRNA of any
259 protein-coding gene is targeted, targeting the region towards the 5' end of the mRNA is
260 preferred because a single cleavage in the 5' end would likely result in the loss of the 5'
261 protective guanosine cap and subsequent degradation of the mRNA by ribonucleases.
262 Instead, if the 3' end of the mRNA is targeted, most of the target mRNA might still be available
263 for some translation to occur, rendering gene knockdown less efficient. In such cases, some
264 truncated proteins may form, whose effects are unpredictable. Therefore, while choosing GS
265 for any mRNA, preference may be given to the sites proximal to the 5' end of the mRNA. In
266 this study, we chose to target human 28S rRNA, which is the most abundant RNA species
267 and a non-coding RNA.
268 After choosing a target site, a GS should be designed, containing a sequence
269 complementary to the target site and either RCCA or NCCA at the 3' end [15, 46-48]. The
270 presence of CCA at the 3' end of GS is critical for efficient cleavage but not required for
271 cleavage [24]. Although all three nucleotides are very critical, CC (two cytosines) are more
272 critical than A in determining the cleavage efficiency, but they are not important for cleavage
273 site selection [24].
274
275 **Prediction of M1GS target sites for human 28S rRNA**
276 To demonstrate that the bioinformatic tool we designed works as expected, we used it to
277 identify M1GS target sites in the human 28S rRNA sequence. A primary reason to choose to
278 target 28S rRNA is to propose M1GS-mediated rRNA downregulation as a potential anticancer
279 modality for cancers in which 45S rRNA genes are upregulated [31-33] and RNA Pol I
280 transcription has been therapeutically targeted [34-40]. The understanding has been that
281 reduced protein synthesis in the cancer cells would result in antiproliferation effects.
282 Furthermore, among different rRNAs, we chose 28S because it possesses catalytic activity
283 that forms peptide bonds between amino acids during protein synthesis.
284 We obtained a publicly available 28S rDNA sequence (GenBank accession number:
285 KY962518.1) (Figure S3), converted it to the corresponding RNA sequence, and provided it
286 as the input sequence in the tool. We started with stringent input options. For the nucleotide
287 at the -1 position, pyrimidines (C and U) were selected, and for the nucleotide at the +1
288 position, purine (G) was selected. Lastly, an unpaired CCA at the 3' end and an unpaired
289 nucleotide at the -1 position were opted for. The output listed multiple target sites, of which
290 one at position 2862 (Figure 3, enclosed by a red rectangle) was used to generate a guide

291 sequence of 15 nt for cleaving 28S rRNA. A reason to pick this target site is that it is located
292 close to the center of the 28S rRNA sequence. The notion is that if we cleave 28S rRNA right
293 in the middle, maximum damage to the RNA can be inflicted, and, relatively, it is easier to
294 design suitable primers for qPCR analysis of the target region. Next, we demonstrate that the
295 tool provides more target sites for 28S rRNA in the output if we relax some input options. For
296 example, when we excluded the requirement of unpaired CCA at the 3' end and an unpaired
297 nucleotide at the -1 position, the output listed more target sites than before (compare outputs
298 of Figure 3 with Figure S4).
299
300 **M1GS-mediated downregulation of 28S rRNA in a lung cancer cell line**
301 The GS of 15 nt designed to target 28S rRNA was fused to wild-type M1 RNA (hereafter
302 referred to as $M1GS^{28SrRNA}$) or enzymatically inactive mutant M1 RNA (hereafter referred to as
303 $\Delta M1GS^{28SrRNA}$), which served as a negative control to delineate the antisense effects, if any,
304 that could arise due to base-pairing of the GS with the target RNA [9, 23]. A cartoon depicting
305 different elements of the designed M1GS constructs is given in Figure S5A. M1GS can be
306 expressed either with a 3' overhang (Figure S5B) or without a 3' overhang sequence by
307 inserting a self-cleaving hammerhead ribozyme at the 3' end of GS (Figure S5C). DNA
308 sequences of M1GS cassettes, sequence alignment of the active and inactive M1 RNAs, and
309 a PCR assay to differentiate the active and inactive M1 RNAs are provided in Figure S6.
310 Usage of a self-cleaving hammerhead ribozyme at the 3' end of the GS has been
311 recommended for an efficient cleavage because additional sequences downstream of the 3'
312 CCA sequence lower the cleavage rate of the substrates by M1 RNA [23]. We introduced a
313 self-cleaving hammerhead (HH) ribozyme [27], downstream of the M1GS, to ensure a free 3′
314 end for efficient cleavage of the 28S rRNA by the $M1GS^{28SrRNA}$. We transfected the human
315 lung cancer cell line A549 with $M1GS^{28SrRNA}$ and $\Delta M1GS^{28SrRNA}$ in two biological replicates.
316 Following transfection, DNA-free RNA was obtained and used to perform quantitative PCR
317 (qPCR) and semiquantitative RT-PCR assays for 28S rRNA, M1GS RNAs, and internal
318 controls. Non-transfected cells were used as controls.
319 The qPCR assay results showed a significant reduction in the levels of 28S rRNA in
320 $M1GS^{28SrRNA}$-expressing cells compared to $\Delta M1GS^{28SrRNA}$-expressing and the non-transfected
321 cells (Figure 4A). In both biological replicates, we found 28S rRNA downregulation, but in one
322 replicate we observed greater 28S rRNA reduction than the other. We used the averages of
323 the two biological replicates for a box plot analysis (Figure 4A). To further confirm the results,
324 we carried out a semiquantitative RT-PCR assay using cDNA from the biological replicate
325 which showed a greater reduction of 28S rRNA (Figure 4B). We observed similar reduction of
326 28S rRNA, not GAPDH (an internal control), in the transfected cells expressing the active
327 $M1GS^{28SrRNA}$ compared to the cells expressing $\Delta M1GS^{28SrRNA}$ or the non-transfected cells

328 (Figure 4B, image panels 1-4). We confirmed successful transfection of the cells through DNA
329 PCR amplification of both M1GSs and GAPDH (as a control) (Figure 4B, image panels 5-6),
330 and a separate RT-PCR assay to confirm the expression of both M1GSs (Figure 4B, image
331 panels 7-8 & 9-10), and GAPDH controls (Figure 4B, image panels 13-14). Further, we
332 demonstrated self-cleavage of the HH ribozyme that was part of the M1GS constructs (Figure
333 4B: For $M1GS^{28SrRNA}$, compare gel panel 7, lane 3 with panel 11, lane 3. For $\Delta M1GS^{28SrRNA}$,
334 compare gel panel 9, lane 2 with panel 11, lane 2). We also assayed for M1GS expression
335 using qPCR (Figure S7). Both RT-PCR and qPCR data (Figure 4B and Figure S7) revealed
336 that $\Delta M1GS^{28SrRNA}$ is expressed at higher levels than the $\Delta M1GS^{28SrRNA}$ in the transfected cells.
337 It appears that, with transient transfections, the expression levels of the constructs are
338 inconsistent, which also explains the differential downregulation of 28S rRNA between the two
339 biological replicates. So, these results indicate that higher reductions of 28S rRNA are likely
340 possible with increased expression levels of $M1GS^{28SrRNA}$.
341
342 **Further validation of the *M1GS target site finder* tool**
343 We tested our tool to validate target sites for two previously published target RNAs that were
344 cleaved by customized M1GSs. One of the targets was the thymidine kinase (TK) mRNA of
345 the human herpes simplex virus 1 (HSV-1) [23]. The gene sequence and a screenshot of the
346 output showing a list of M1GS targets sites identified by the tool are provided in Figure S8, in
347 which the site enclosed in a red rectangle was used in the study [23].
348 The other target we tested is the 5' UTR of the hepatitis C virus (HCV) [25]. For this
349 target RNA, we used both RNAfold and Mfold software to predict the secondary structure of
350 the HCV RNA. The results demonstrate that different software provide different secondary
351 structure predictions for the same RNA sequence (Figure S9). For example, for a 13 nt GS,
352 when Mfold or RNAfold-predicted secondary structure was fed to the tool with a requirement
353 of ≥ 7 nt in a single-stranded form, the tool did not find any target sites. With a requirement of
354 6 nt to be in the single-stranded form, when the secondary structure as predicted by the Mfold
355 software was fed to the tool, it provided two target sites, including the one that was used in
356 the previous study to design a GS to cleave the target RNA (Figure S9B) [25]. However, for
357 the same input options, when the secondary structure predicted by RNAfold was fed to the
358 tool, no M1GS target sites were identified by the tool because, according to the RNAfold
359 prediction, target sites with a stretch of 6 nt or less (all the way to 1 nt) do not exist in a single-
360 stranded form (Figure S9C). However, for the same RNAfold-predicted secondary structure,
361 when the input of single-stranded form requirement of the target RNA was set to '0', the tool
362 predicted three M1GS target sites, including the one used in the study (Figure S9D) [25].
363
364

365 **Discussion**

366 We describe here a user-friendly Python script-based bioinformatic tool we designed to identify
367 M1GS cleavage sites in any target RNA. Overall, the tool offers various options for selecting
368 GS features as per the recommended parameters to optimally meet M1GS requirements and
369 users' choices to experiment with. The tool has been made publicly available for use and a
370 link to access it is provided below.

371 Human rRNA undergoes more than 200 modifications, of which some are reported to
372 be altered in multiple cancers. Examples include pseudouridylation and 2'-O-methylation [50-
373 52]. It remains to be tested if any of these or other rRNA modifications near the cleavage site
374 in the target RNA have any impact on M1GS cleavage. Such studies would enable the
375 incorporation of more features into the bioinformatic tool described here. For example, if any
376 of the rRNA modifications negatively impact M1GS cleavage, the tool can be linked to
377 available databases of rRNA modifications in both cancerous and non-cancerous cells to avoid
378 target regions around sites carrying potentially impeding rRNA modifications. Similarly, the
379 tool can be further linked to the human transcriptome of specific cell types to avoid potential
380 off-targets. We have deposited the script on GitHub
381 (https://github.com/navinfreeze/m1gstargetfinder), which we permit for unrestricted download
382 and modification as deemed necessary by users.

383 Customized ribozymes have seldom been used as gene-targeting tool or antiviral
384 agents, despite their versatile utility [25, 53, 54]. We hope that the availability of a user-friendly
385 bioinformatic tool to identify M1GS target sites would encourage more users to employ the
386 M1GS tool in RNA-cleaving/reverse genetic studies and to further modify the tool as more
387 data emerge on M1GS functionality.

388 Of note, M1GS has not been previously used to downregulate RNA as abundant as
389 rRNA, which constitutes ~ 80% of total RNA in human cells [55]. Therefore, the efficient
390 downregulation of abundant 28S rRNA observed in this study suggests a high turnover
391 number for the M1GS ribozyme. In comparison, the available RNA-cleaving tools, RNAi and
392 Cas13a, have a modest turnover number of ~10 [56, 57]. Therefore, our findings hold a
393 promise in developing the M1GS as the most potent RNA-cleaving tool. Further, compared
394 with the RNA interference (RNAi) and other gene-targeting strategies, M1GS ribozymes offer
395 several advantages. One is that they cleave the target RNA without the need to introduce any
396 additional protein cofactors [19, 58, 59]. On the other hand, RNAi, for example, requires
397 several cellular factors, such as Exportin V, Dicer, and Argonaute proteins, for small interfering
398 RNA (siRNA)-mediated gene silencing [60].

399 Furthermore, several viruses have evolved counter-defense mechanisms to block
400 RNAi-mediated host defense responses [61, 62]. By contrast, viruses lack counter-defense
401 mechanisms against engineered ribozymes as they don't encounter them naturally during

402 infections. Moreover, modulation of ribozyme expression levels is simpler than that of the other
403 RNA-cleaving tools, as it requires expression of only one component. On the other hand, RNAi
404 and CRISPR-Cas-based systems require simultaneous modulation of multiple components.
405 Further experiments are needed to determine whether M1GS-mediated
406 downregulation of rRNA exhibits anti-cancer activity in cancers where rRNA is upregulated.
407 Direct downregulation of rRNA, if proven successful in exhibiting anticancer activity, may serve
408 as a better viable alternative to targeting RNA pol I, because RNA pol I transcription may be
409 necessary for other cellular functions [63].
410 The next concern is the *in vivo* delivery of M1GS constructs. Notably, previous studies
411 have demonstrated the feasibility of systemic delivery of M1GS-containing plasmids in virus-
412 infected mouse models using attenuated bacteria, and successfully cleaved the target viral
413 RNA, resulting in reduced viral infections [64, 65].
414 Lastly, a question of interest has been, how does M1GS of bacterial origin work so
415 efficiently in human cells? Is any human protein(s) involved in aiding M1GS cleavage of the
416 target RNA? These interesting questions remain to be answered.
417
418 **Methods**
419 **Prediction of the target RNA secondary structure**
420 If the secondary structure of the target RNA is not provided by the user in the Vienna format
421 in the form of ".", "(", ")") as input, the tool uses secondary structure predictions provided from
422 the RNAfold webserver (http://rna.tbi.univie.ac.at/cgibin/RNAWebSuite/RNAfold.cgi) [66]. The
423 default RNAfold settings are used to predict secondary structure, and these settings are listed
424 in Figure S2.
425
426 **The web interface**
427 The web interface for the tool was developed using Python3 and Django 3.1.6. The web
428 interface mainly consists of two sections: the inputs and the output. To find the target sites,
429 the interface runs the program in the background, and the time required for this task varies
430 depending on the size of the target RNA. Once this task is over, the tool loads the output
431 above 'the inputs' section. The M1GS target site finder tool can be accessed at the following
432 link http://m1gstargetfinder.bits-hyderabad.ac.in:8000/m1gs/.
433
434 **Plasmid construction**
435 The M1GS expression cassettes designed to target human 28S rRNA consisted of H1
436 promoter, followed by wildtype (active) or mutant (inactive) M1 RNA, a linker region, a 15 bp
437 guide sequence (GS) (5'-GCCAATCCTTATCCC-3'), and a self-cleaving hammerhead
438 ribozyme (HH) (Fig. S5). The GS was designed to cleave 28S rRNA at between nts 2862 and

439 2863, a target site identified by the bioinformatic tool. These expression cassettes were
440 commercially synthesised (ABclonal), and then cloned into a pRS retroviral vector using EcoRI
441 and XhoI restriction sites. Plasmid DNA from the positive clones was isolated using *QIAprep*
442 *Spin Miniprep Kit* (Qiagen), and the presence of the M1GS constructs was verified by PCR
443 amplification of the active and inactive M1 DNA using specific primers.
444
445 **Human cell culture**
446 The human lung cancer cell line A549 (ATCC CCL-185) was purchased from the American
447 Type Culture Collection (Manassas, VA, USA). The cells were cultured in Dulbecco's Modified
448 Eagle Medium (DMEM) (HiMedia), supplemented with 10% (v/v) fetal bovine serum (HiMedia)
449 and 1% (w/v) penicillin streptomycin (HiMedia), at 37°C in a humidified incubator with 5% CO_2.
450 The medium was changed every 2 days until the cells reached 70–80% confluence. For
451 detaching the cells during passages, 0.25% (w/v) Trypsin-EDTA (HiMedia) was used.
452
453 **Transfection**
454 Transient transfection of A549 cells was performed using JetPRIME® kit (PolyPlus). Once the
455 cells in a 6-well plate reached 70-80% confluency, a transfection master mix consisting of 2
456 μg plasmid DNA containing active (pRS-M1GS^{28SrRNA}) or inactive M1GS (pRS-ΔM1GS^{28SrRNA})
457 and 4 µl of JetPrime reagent (1:2 ratio) in 200 µL of JetPrime® buffer (PolyPlus) was added
458 for each well and then the cells were incubated at 37°C for 24 h. For transfection, the cells
459 were seeded at a density of 2,50,000 cells per well in a 6-well plate. After transfection, cells
460 were supplemented with additional media. The cells were harvested 24 h post-transfection
461 and processed immediately for RNA and DNA isolation.
462
463 **DNA and RNA isolation and semiquantitative reverse transcription (RT)-PCR**
464 Total DNA and RNA were isolated from the control and transfected cell lines using the *AllPrep*
465 *DNA/ RNA/Protein Mini Kit* (Qiagen). To confirm the presence of the M1GS constructs in the
466 transfected cells, PCR amplification of M1GS constructs and the endogenous glyceraldehyde-
467 3-phosphate dehydrogenase (GAPDH) gene (as an internal control) was carried using initial
468 denaturation for 2 min at 95°C, followed by 30 cycles of 30 sec at 95°C, 30 sec at 58°C, and
469 30 sec at 72°C, and a final extension for 3 min at 72°C, in the presence of *GoTaq® Green*
470 *Master Mix* (Promega).
471 The isolated total RNA was treated with *Turbo DNA-free* kit (Invitrogen) to eliminate
472 any contaminating genomic DNA. One μg of DNA-free RNA was reverse transcribed to cDNA
473 using *SuperScript III First Strand cDNA synthesis* kit (Invitrogen). One μl (cDNA from ~50 ng
474 DNA-free RNA) of reverse transcribed product was then used for PCR amplification of the

475 active and the inactive M1GS ribozymes, the HH ribozyme, and GAPDH control with initial
476 denaturation for 2 min at 95°C, followed by 25 cycles of 30 sec at 95 °C, 30 sec at 58 °C, and
477 30 sec at 72 °C, and a final extension for 3 min at 72 °C. The same PCR profile was used for
478 amplification of 28S rRNA, but for 23 cycles. For all semiquantitative RT-PCR reactions, RT-
479 negative controls were included.
480
481 **Quantitative PCR (pPCR) assays**
482 The qPCR assays were performed using a *Step One Plus* real-time PCR system (Applied
483 Biosystems) in the presence of *TB Green® Premix Ex Taq*™ (Tli RNase H Plus) (Takara).
484 The qPCR amplification was performed using an initial denaturation at 95 °C for 10 sec,
485 followed by 40 cycles of 15 sec at 95 °C and 60 sec at 60 °C. The relative gene expression
486 levels of 28S RNA and M1GS were calculated using the 2^(-△△CT) method (Livak &
487 Schmittgen, 2001) by normalizing their expression levels to the expression levels of GAPDH
488 as a reference gene. qPCR was performed in duplicates for each sample. Primer sequences
489 used to amplify 28S rRNA span the M1GS cleavage site (2862). All the primers used in this
490 study are listed in Figure S10.
491
492 **Statistical analysis**
493 Data from two technical replicates from two biological replicates were used for all the
494 calculations and data analysis. The qPCR data were used to generate a boxplot. The standard
495 two-tailed t-test was used to analyze significant differences in the gene expression levels
496 between the control (non-transfected) and the transfected cells expressing active or inactive
497 M1GS. A p of < 0.05 was considered statistically significant.
498
499 **Web tools for sequence alignments**
500 Alignment of the active and the inactive M1 RNA sequences was carried out using the
501 nucleotide BLAST (blastn) tool from NCBI
502 (https://blast.ncbi.nlm.nih.gov/Blast.cgi?PROGRAM=blastn&BLAST_SPEC=GeoBlast&PAG
503 E_TYPE=BlastSearch).
504
505 **Other software used.**
506 Figures were made using the free version of Figma software and the licensed version of
507 PowerPoint.
508
509 **Acknowledgements**
510 We profusely thank Dr. Venkat Gopalan and Dr. Lien Lai, The Ohio State University (USA),
511 for their valuable support in sharing reagents, expertise, and critique of the manuscript. We

are also thankful to the CCIT division and the department of Biological Sciences and BITS-Pilani Hyderabad campus, for their support.

Author Contributions: N.P., N.V.P, H.P., S.B., and G.M. designed research, N.P., N.V.P., and H.P. carried out research, N.P., N.V.P., H.P., and G.M. analyzed data, N.P., N.V.P., H.P., and G.M. wrote the manuscript. All authors reviewed the manuscript.

FUNDING

G.M. and N.P. are thankful to the Birla Institute of Science and Technology (BITS) Pilani, Hyderabad campus, for the research grant as part of Centre for Human Disease Research and an Institute Fellowship to N.P. G.M. is also thankful to the Science and Engineering Research Board (SERB) and Anusandhan National Research Foundation (ANRF), Government of India, for the Ramanujan Fellowship (SB-S2-RJN-062-2017) and ARG research grants (ANRF/ARG/2025/000377/LS). N.P. is thankful to the Indian Council of Medical Research (ICMR), Government of India, for Senior Research Fellowship (F.No.2021-13491/GTGE-BMS). N.V.P. is thankful for the internship as part of the Scientific Social Responsibility (SSR) component of CRG grant (CRG/2020/002855) awarded to G.M. H.P is thankful to the Department of Science and Technology, Government of India, for INSPIRE-Junior Research Fellowship (IF240211).

Conflict of interest

The authors declare no conflict of interest.

REFERENCES

1. Arechavala-Gomeza, V. and A. Garanto, *Antisense RNA therapeutics: a brief overview.* Antisense RNA Design, Delivery, and Analysis, 2022: p. 33-49.
2. Chery, J., *RNA therapeutics: RNAi and antisense mechanisms and clinical applications.* Postdoc journal: a journal of postdoctoral research and postdoctoral affairs, 2016. **4**(7): p. 35.
3. Davidson, B.L. and P.B. McCray Jr, *Current prospects for RNA interference-based therapies.* Nature Reviews Genetics, 2011. **12**(5): p. 329-340.
4. Isenmann, M., et al., *Basic Principles of RNA Interference: Nucleic Acid Types and In Vitro Intracellular Delivery Methods.* Micromachines, 2023. **14**(7): p. 1321.
5. Puerta-Fernández, E., et al., *Ribozymes: recent advances in the development of RNA tools.* FEMS microbiology reviews, 2003. **27**(1): p. 75-97.
6. Terns, M.P., *CRISPR-based technologies: impact of RNA-targeting systems.* Molecular cell, 2018. **72**(3): p. 404-412.
7. Gunitseva, N., et al., *RNA-Dependent RNA Targeting by CRISPR-Cas Systems: Characterizations and Applications.* Int J Mol Sci, 2023. **24**(8).
8. Gopalan, V., N. Jarrous, and A.S. Krasilnikov, *Chance and necessity in the evolution of RNase P.* RNA, 2018. **24**(1): p. 1-5.

9. Gopalan, V., A. Vioque, and S. Altman, *RNase P: variations and uses.* Journal of Biological Chemistry, 2002. **277**(9): p. 6759-6762.
10. Esakova, O. and A.S. Krasilnikov, *Of proteins and RNA: the RNase P/MRP family.* Rna, 2010. **16**(9): p. 1725-1747.
11. Evans, D., S.M. Marquez, and N.R. Pace, *RNase P: interface of the RNA and protein worlds.* Trends in biochemical sciences, 2006. **31**(6): p. 333-341.
12. Jarrous, N. and V. Gopalan, *Archaeal/eukaryal RNase P: subunits, functions and RNA diversification.* Nucleic Acids Res, 2010. **38**(22): p. 7885-94.
13. Lai, L.B., et al., *Unexpected diversity of RNase P, an ancient tRNA processing enzyme: challenges and prospects.* FEBS Lett, 2010. **584**(2): p. 287-96.
14. Klemm, B.P., et al., *The diversity of ribonuclease P: protein and RNA catalysts with analogous biological functions.* Biomolecules, 2016. **6**(2): p. 27.
15. Liu, F. and S. Altman, *Ribonuclease P*. 1 ed. Protein Reviews, ed. M.Z. Arassi. Vol. 10. 2010, Verlag Springer New York, NY. XVI, 283.
16. Altman, S., et al., *Enzymatic cleavage of RNA by RNA.* Trends in Biochemical Sciences, 1986. **11**(12): p. 515-518.
17. Kole, R. and S. Altman, *Reconstitution of RNase P activity from inactive RNA and protein.* Proceedings of the National Academy of Sciences, 1979. **76**(8): p. 3795-3799.
18. Vioque, A. and S. Altman, *Ribonuclease P*. 2001: Oxford: Elservier Science.
19. Guerrier-Takada, C., et al., *The RNA moiety of ribonuclease P is the catalytic subunit of the enzyme.* Cell, 1983. **35**(3): p. 849-857.
20. Forster, A.C. and S. Altman, *External guide sequences for an RNA enzyme.* Science, 1990. **249**(4970): p. 783-786.
21. Jarrous, N. and F. Liu, *Human RNase P: overview of a ribonuclease of interrelated molecular networks and gene-targeting systems.* RNA, 2023. **29**(3): p. 300-307.
22. Trang, P., K. Kim, and F. Liu, *Developing RNase P ribozymes for gene‐targeting and antiviral therapy.* Cellular microbiology, 2004. **6**(6): p. 499-508.
23. Liu, F. and S. Altman, *Inhibition of viral gene expression by the catalytic RNA subunit of RNase P from Escherichia coli.* Genes & development, 1995. **9**(4): p. 471-480.
24. Liu, F. and S. Altman, *Requirements for cleavage by a modified RNase P of a small model substrate.* Nucleic acids research, 1996. **24**(14): p. 2690-2696.
25. Mao, X., et al., *Inhibition of hepatitis C virus by an M1GS ribozyme derived from the catalytic RNA subunit of Escherichia coli RNase P.* Virology journal, 2014. **11**: p. 1-9.
26. Trang, P., et al., *Effective inhibition of human cytomegalovirus gene expression and replication by a ribozyme derived from the catalytic RNA subunit of RNase P from Escherichia coli.* Proceedings of the National Academy of Sciences, 2000. **97**(11): p. 5812-5817.
27. Ujor, V.C., et al., *Ribozyme-Mediated downregulation uncovers DNA integrity scanning protein A (DisA) as a solventogenesis determinant in Clostridium beijerinckii.* Frontiers in bioengineering and biotechnology, 2021. **9**: p. 669462.
28. Gao, Z., et al., *Engineered miniature H1 promoters with dedicated RNA polymerase II or III activity.* J Biol Chem, 2021. **296**: p. 100026.
29. Henriksen, J.R., et al., *Comparison of RNAi efficiency mediated by tetracycline-responsive H1 and U6 promoter variants in mammalian cell lines.* Nucleic Acids Res, 2007. **35**(9): p. e67.
30. Trang, P., et al., *A ribozyme derived from the catalytic subunit of RNase P from Escherichia coli is highly effective in inhibiting replication of herpes simplex virus 1.* Journal of molecular biology, 2000. **301**(4): p. 817-826.
31. Uemura, M., et al., *Overexpression of ribosomal RNA in prostate cancer is common but not linked to rDNA promoter hypomethylation.* Oncogene, 2012. **31**(10): p. 1254-1263.
32. Zhou, H., et al., *Overexpression of ribosomal RNA in the development of human cervical cancer is associated with rDNA promoter hypomethylation.* PLoS One, 2016. **11**(10): p. e0163340.

33. Tsoi, H., et al., *Pre-45s rRNA promotes colon cancer and is associated with poor survival of CRC patients.* Oncogene, 2017. **36**(44): p. 6109-6118.
34. Bywater, M.J., et al., *Inhibition of RNA polymerase I as a therapeutic strategy to promote cancer-specific activation of p53.* Cancer cell, 2012. **22**(1): p. 51-65.
35. Ferreira, R., et al., *Targeting the RNA polymerase I transcription for cancer therapy comes of age.* Cells, 2020. **9**(2): p. 266.
36. Hannan, K.M., et al., *Dysregulation of RNA polymerase I transcription during disease.* Biochimica Et Biophysica Acta (BBA)-Gene Regulatory Mechanisms, 2013. **1829**(3-4): p. 342-360.
37. Low, J.Y., et al., *Effective targeting of RNA polymerase I in treatment-resistant prostate cancer.* The Prostate, 2019. **79**(16): p. 1837-1851.
38. Wei, T., et al., *Small-molecule targeting of RNA polymerase I activates a conserved transcription elongation checkpoint.* Cell reports, 2018. **23**(2): p. 404-414.
39. El Hassouni, B., et al., *CX-5461 inhibits pancreatic ductal adenocarcinoma cell growth, migration and induces DNA damage.* Molecules, 2019. **24**(24): p. 4445.
40. Drygin, D., et al., *Targeting RNA polymerase I with an oral small molecule CX-5461 inhibits ribosomal RNA synthesis and solid tumor growth.* Cancer research, 2011. **71**(4): p. 1418-1430.
41. Zahler, N.H., E.L. Christian, and M.E. Harris, *Recognition of the 5' leader of pre-tRNA substrates by the active site of ribonuclease P.* Rna, 2003. **9**(6): p. 734-745.
42. Brännvall, M., B.M. Fredrik Pettersson, and L.A. Kirsebom, *The residue immediately upstream of the RNase P cleavage site is a positive determinant.* Biochimie, 2002. **84**(8): p. 693-703.
43. Cobaleda, C. and I. Sánchez-Garcıa, *In vivo inhibition by a site-specific catalytic RNA subunit of RNase P designed against the BCR-ABL oncogenic products: a novel approach for cancer treatment.* Blood, The Journal of the American Society of Hematology, 2000. **95**(3): p. 731-737.
44. Toumpeki, C., et al., *Construction of an M1GS ribozyme for targeted and rapid mRNA cleavage; application on the Ets-2 oncogene.* Medicinal Chemistry, 2018. **14**(6): p. 604-616.
45. Liu, Y., et al., *Suppressing Kaposi's Sarcoma-Associated Herpesvirus Lytic Gene Expression and Replication by RNase P Ribozyme.* Molecules, 2023. **28**(8): p. 3619.
46. Frank, D.N., M.E. Harris, and N.R. Pace, *Rational design of self-cleaving pre-tRNA-ribonuclease P RNA conjugates.* Biochemistry, 1994. **33**(35): p. 10800-8.
47. Lundblad, E.W. and S. Altman, *Inhibition of gene expression by RNase P.* N Biotechnol, 2010. **27**(3): p. 212-21.
48. Su, Y.Z., et al., *In vitro construction of effective M1GS ribozymes targeting HCMV UL54 RNA segments.* Acta Biochim Biophys Sin (Shanghai), 2005. **37**(3): p. 210-4.
49. Zhu, J., et al., *Structural and mechanistic basis for recognition of alternative tRNA precursor substrates by bacterial ribonuclease P.* Nat Commun, 2022. **13**(1): p. 5120.
50. Barozzi, C., et al., *Alterations of ribosomal RNA pseudouridylation in human breast cancer.* NAR Cancer, 2023. **5**(2): p. zcad026.
51. Jasinski-Bergner, S., et al., *Relevance of 2'-O-Methylation and Pseudouridylation for the Malignant Melanoma.* Cancers (Basel), 2021. **13**(5).
52. Taoka, M., et al., *Landscape of the complete RNA chemical modifications in the human 80S ribosome.* Nucleic Acids Res, 2018. **46**(18): p. 9289-9298.
53. Shin, K.-S., B.A. Sullenger, and S.-W. Lee, *Ribozyme-mediated induction of apoptosis in human cancer cells by targeted repair of mutant p53 RNA.* Molecular therapy, 2004. **10**(2): p. 365-372.
54. Trujillo, A.J., et al. *A discovery with potential to revitalize hammerhead ribozyme therapeutics for treatment of inherited retinal degenerations*. in *Retinal Degenerative Diseases: Mechanisms and Experimental Therapy*. 2019. Springer.
55. Choy, J.Y., et al., *A resource of ribosomal RNA-depleted RNA-Seq data from different normal adult and fetal human tissues.* Sci Data, 2015. **2**: p. 150063.

56. Feng, Z.Y., et al., *Impact of Divalent Metal Ions on Regulation of Trans-Cleavage Activity of CRISPR-Cas13a: A Combined Experimental and Computational Study.* Chembiochem, 2023. **24**(10): p. e202300034.
57. Hutvágner, G. and P.D. Zamore, *A microRNA in a multiple-turnover RNAi enzyme complex.* Science, 2002. **297**(5589): p. 2056-60.
58. Kruger, K., et al., *Self-splicing RNA: autoexcision and autocyclization of the ribosomal RNA intervening sequence of Tetrahymena.* cell, 1982. **31**(1): p. 147-157.
59. Grassi, G. and J.C. Marini, *Ribozymes: structure, function and potential therapy for dominant genetic disorders.* Annals of medicine, 1996. **28**(6): p. 499-510.
60. Wilson, R.C. and J.A. Doudna, *Molecular mechanisms of RNA interference.* Annual review of biophysics, 2013. **42**: p. 217-239.
61. Csorba, T., L. Kontra, and J. Burgyán, *viral silencing suppressors: Tools forged to fine-tune host-pathogen coexistence.* Virology, 2015. **479-480**: p. 85-103.
62. Li, H.W. and S.W. Ding, *Antiviral silencing in animals.* FEBS Lett, 2005. **579**(26): p. 5965-73.
63. Wong, L.H., et al., *Corrigendum: Centromere RNA is a key component for the assembly of nucleoproteins at the nucleolus and centromere.* Genome Res, 2024. **34**(6): p. 979-980.
64. Bai, Y., et al., *Oral delivery of RNase P ribozymes by Salmonella inhibits viral infection in mice.* Proceedings of the National Academy of Sciences, 2011. **108**(8): p. 3222-3227.
65. Bai, Y., et al., *Salmonella-mediated delivery of RNase P-based ribozymes for inhibition of viral gene expression and replication in human cells.* Proceedings of the National Academy of Sciences, 2010. **107**(16): p. 7269-7274.
66. Gruber, A.R., et al., *The vienna RNA websuite.* Nucleic acids research, 2008. **36**(suppl_2): p. W70-W74.

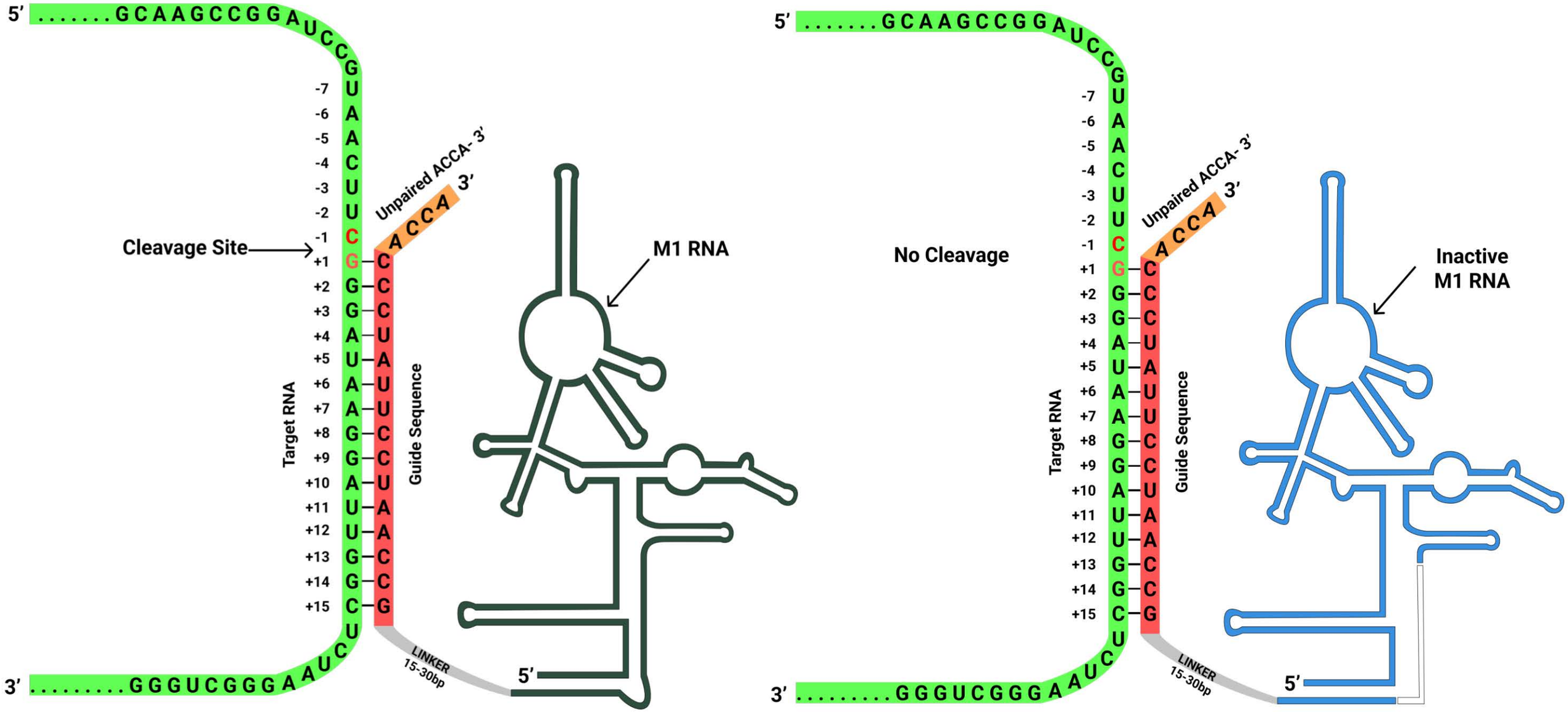

Figure 1: A schematic representation of the M1GS strategy to cleave a target RNA.
The cartoon shows how the engineered RNase P ribozyme M1GS cleaves the target RNA by hybridizing to it through a complementary guide sequence (GS). Human 28S rRNA as a target RNA and the corresponding complementary guide sequence (GS) are shown in the diagram. The diagram on the left represents M1GS with an active M1 RNA and the one on the right represents M1GS with an inactive, mutant M1 RNA.

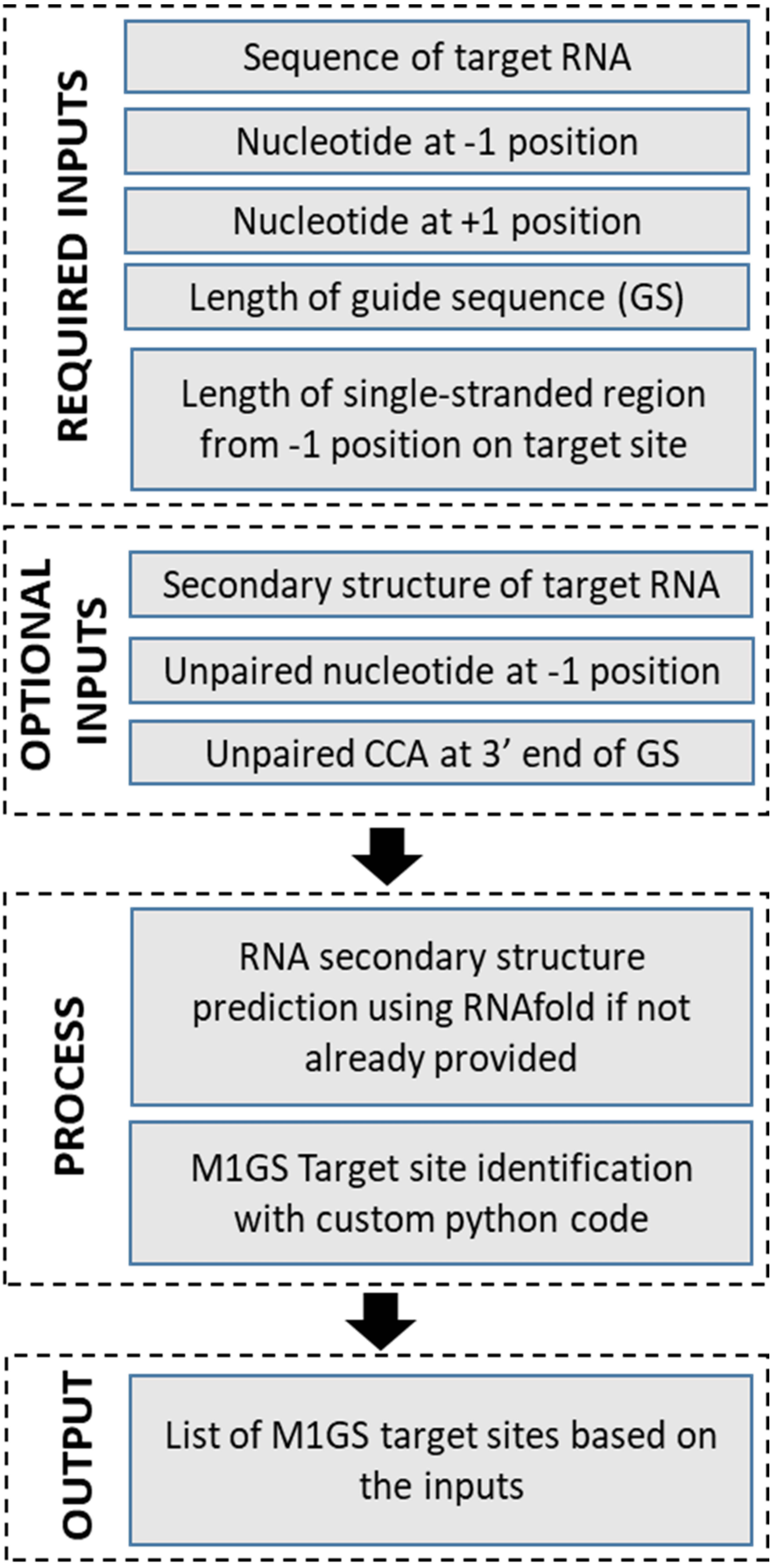

Figure 2: The flowchart depicts the operational modality of the *M1GS Target site finder* tool.

Input

DNA or RNA sequence of the target RNA

CTCCCGGCGCCCACCCCCGCGGGGAATCCCCCGCGAGGGGGGTCTCCCCCGCGGGGGCGCGCCGGCGTCT
CCTCGTGGGGGGGCCGGGCCACCCCTCCCACGGCGCGACCGCTCTCCCACCCCTCCTCCCCGCGCCCCCG
CCCCGGCGACGGGGGGGGTGCCGCGCGCGGGTCGGGGGGCGGGGCGGACTGTCCCCAGTGCGCCCCGGGC
GGGTCGCGCCGTCGGGCCCGGGGGGAGGTTCTCTCGGGGCCACGCGCGCGTCCCCCGAAGAGGGGGACGG

NOTE:

If you want to use your own secondary structure, please paste the secondary structure of your target sequence in the vienna format. If you do not have one, a secondary structure predicted by the RNAFold Software will be used.

Example: ((....))(((((((.....))))).....)))......((....())....)

Secondary structure of the target RNA in Vienna format (Optional)

Enter sequence here

Nucleotide at -1 position — C, U, A, G

Nucleotide at +1 position — G, A

CCA at 3′ position of M1GS unpaired

Unpaired nucleotide at -1 position according to the predicted structure of the target RNA

Desirable length of the target RNA from -1 position that is predicted to exist in a single-stranded form: 7

Length of the Guide Sequence (GS): 15

Results:

Target sites with C at -1

Position of -1 site in the target RNA	Target site sequence (from +1 position)	% GC content
1359	5'-GCACGAAAGCCGCCG-3'	73.3
2862	5'-GGGAUAAGGAUUGGC-3'	53.3
4675	5'-GCCUCUAAGUCAGAA-3'	46.7

Target sites with U at -1

Position of -1 site in the target RNA	Target site sequence (from +1 position)	% GC content
1974	5'-GGAAGUCGGAAUCCG-3'	60.0

Figure 3: Identification of M1GS target sites for human 28S rRNA using the tool.
Screenshot from the *M1GS target site finder* tool that shows input options chosen and output as a list of M1GS target sites for 28S rRNA. The input options chosen here are more stringent than the ones shown in Figure S4.
Note: For better visualization, this figure was created by merging multiple cropped snapshots instead of showing a single snapshot.

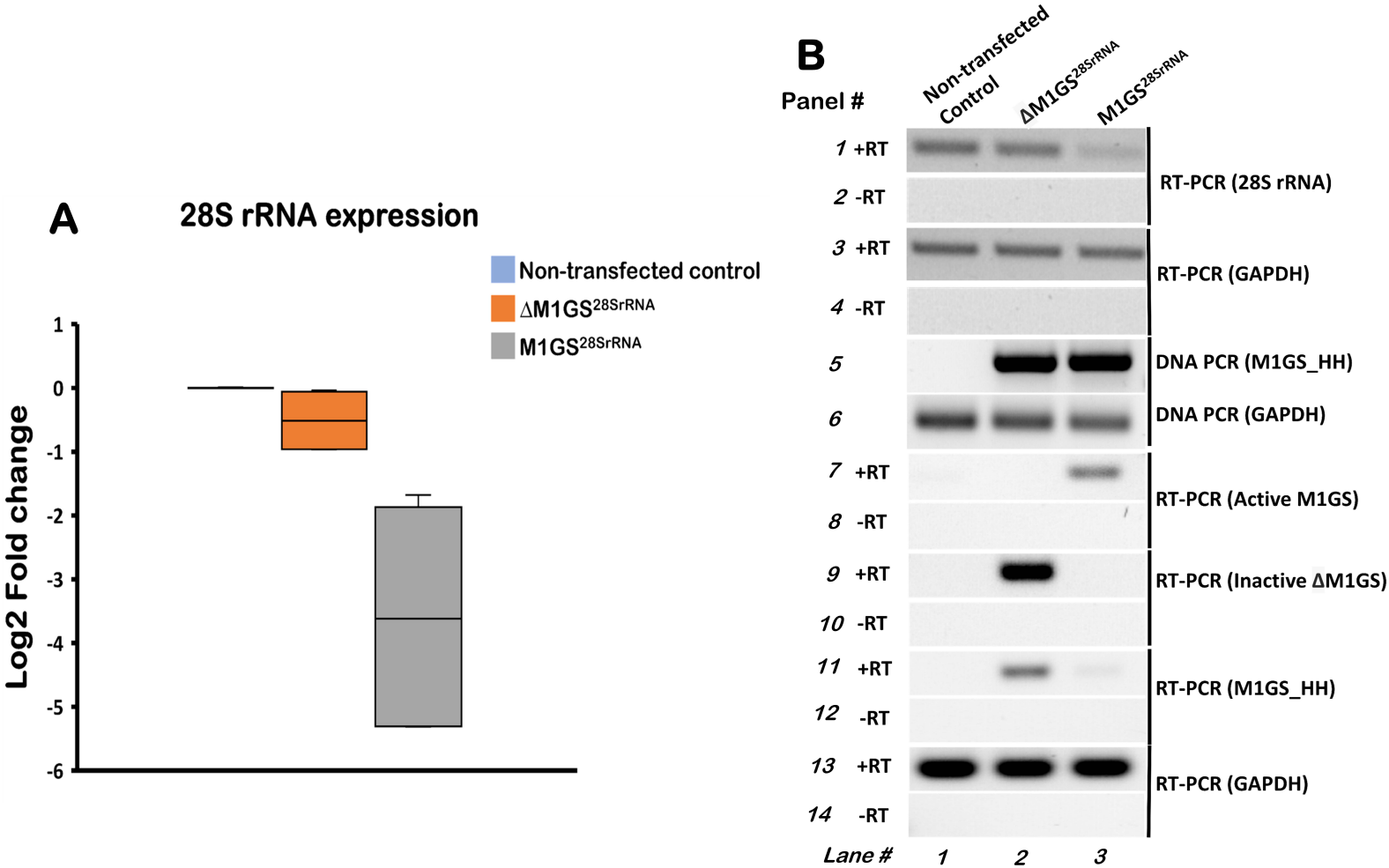

Figure 4: M1GS-mediated downregulation of 28S rRNA in human lung cancer cell line. (A) A box plot analysis of qPCR data depicts relative 28S rRNA levels in human A549 cell line expressing different M1GS constructs and non-transfected controls. 28S rRNA expression levels are normalized to those of non-transfected controls. (B) Gel images show semiquantitative RT-PCR analysis of 28S rRNA and GAPDH, PCR analysis of M1GS constructs and GAPDH, RT-PCR analysis of M1GS, GAPDH, and the hammerhead ribozyme. Primers specific to active and inactive M1GS were used for their amplification.